NANO LETTERS

pubs.acs.org/NanoLett

Letter

Magnetic Stiffening in 3D Cell Culture Matrices

Wen Chen, Ying Zhang, Jyoti Kumari, Hans Engelkamp, and Paul H. J. Kouwer*

Cite This: *Nano Lett.* 2021, 21, 6740–6747

Read Online

ACCESS | Metrics & More | Article Recommendations | Supporting Information

ABSTRACT: The mechanical environment of a cell is not constant. This dynamic behavior is exceedingly difficult to capture in (synthetic) *in vitro* matrices. This paper describes a novel, highly adaptive hybrid hydrogel composed of magnetically sensitive magnetite nanorods and a stress-responsive synthetic matrix. Nanorod rearrangement after application of (small) magnetic fields induces strain in the network, which results in a strong (over 10-fold) stiffening even at minimal (2.5 wt %) nanorod concentrations. Moreover, the stiffening mechanism yields a fast and fully reversible response. In the manuscript, we quantitatively analyze that forces generated by the particles are comparable to cellular forces. We demonstrate the value of magnetic stiffening in a 3D MCF10A epithelial cell experiment, where simply culturing on top of a permanent magnet gives rise to changes in the cell morphology. This work shows that our hydrogels are uniquely suited as 3D cell culture systems with on-demand adaptive mechanical properties.

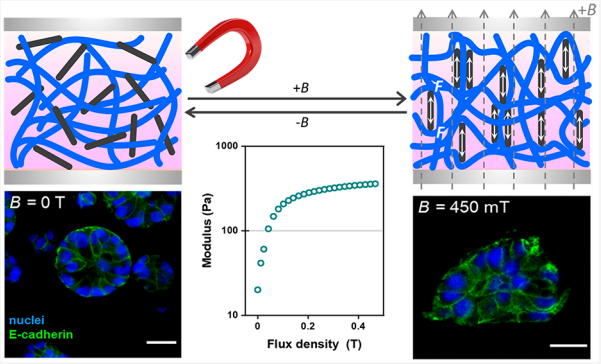

KEYWORDS: *adaptive hydrogels, ferrogels, magnetic iron oxide nanoparticles, extracellular matrices, mammary epithelium*

INTRODUCTION

The cell and its microenvironment are shaped by their mutual dynamic and reciprocal interactions.[1,2] *In vivo*, the local properties of the matrix are not constant but vary in time as a result of cellular protein deposition and remodeling.[3] Recently, new culture systems have been developed, for which the biochemical and biophysical properties can be modulated spatially and temporally, which adds great perspectives for tissue regenerative and disease modeling.[4−6] Strategies based on external stimuli such as pH,[7−9] temperature,[10−13] cross-linking,[14−16] and light[17,18] have been introduced to make the culture systems adaptive. These strategies, however, often lack reversibility, only induce small changes, pose biocompatibility challenges, and/or are restricted to 2D cell experiments.

Over the past decades, magnetic fields have been studied as external cues to tune the mechanical properties of soft hydrogels and tissue culture matrices, since they are biocompatible[19,20] and easily and reversibly applied.[21−23] Researchers demonstrated how magnetically responsive materials alter cell behavior by applying an external field.[19,20,23] Although these reported hydrogel hybrids show potential in adaptive biological applications, they require high loadings of magnetic nanoparticles, which compromise compatibility with 3D cell culture environments.[21,23] Our research question is as follows: Is it possible to truly benefit from the advantages that magnetic fields offer for cell culture applications,[23,24] where we consider sensitivity to the field, reversibility, and tailorability as well as biocompatibility?

In this work, we present a magnetically responsive hydrogel (ferrogel) that, even at low iron oxide nanoparticle concentrations (C < 2.5 wt %) shows a reversible and large—up to an 18-fold stiffness change—at low magnetic fields (200 mT). We study the key parameters that determine the magnitude of the magnetic stiffening response, and we provide insight in forces and stresses at the microscopic scale from where macroscopic stiffening originates. The ferrogel is fully biocompatible and does not contract in magnetic fields, which renders it suitable for 3D cell culture experiments. In addition, we demonstrate the potential of magnetic stiffening in a 3D cell culture study where the mammary epithelial cells change their phenotype after culturing simply on top of a permanent magnet.

RESULTS AND DISCUSSION

Materials. For our experiments, we use synthetic and highly biomimetic polyisocyanide (PIC)-based hydrogels,[25] which share the fibrous architecture and the associated intricate mechanical properties with biological gels, for instance those based on collagen and fibrin.[26] They are, however, fully

Received: January 27, 2021
Revised: August 9, 2021
Published: August 13, 2021

https://doi.org/10.1021/acs.nanolett.1c00371
Nano Lett. 2021, 21, 6740–6747

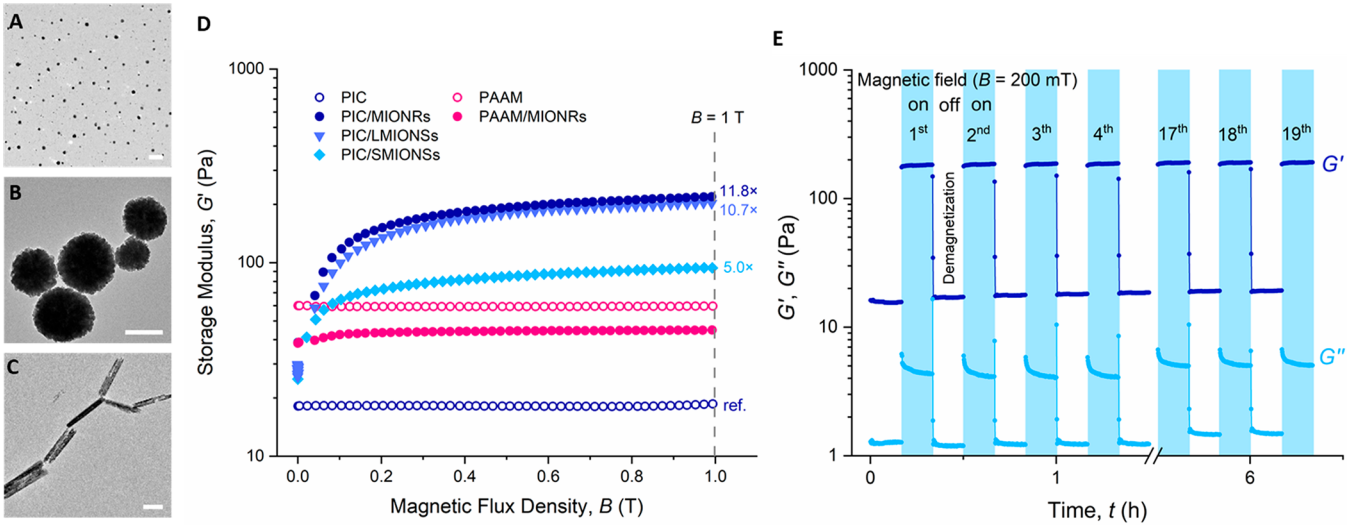

Figure 1. (A–C) TEM images of magnetite nanoparticles: small (SMIONSs, A) and large (LMIONSs, B) spheres and nanorods (MIONRs, C). The scale bars represent 200 nm. (D) Storage modulus G' of hybrid gels (PIC and PAAM) of the three magnetic nanomaterials as a function of magnetic flux density B (conditions: aqueous solutions with nanoparticle concentration of 25 mg mL^{-1}, PIC concentration of 0.5 mg mL^{-1}, T = 37 °C, PAAM concentration of 30 mg mL^{-1}). The stiffening compared to pure PIC at B = 1 T is indicated. (E) Magnetic stiffening is fast and reversible, indicated by 19 cycles of 20 min each (10 min field on, 10 min off). Conditions: the concentrations of PIC and MIONRs are 0.5 and 25 mg mL^{-1}, respectively. Data points are recorded every 6 s.

Scheme 1. (A–C) Schematic Overview of the Magnetic Stiffening Process[a] and (D) Schematic Representation of a Magnetorheological Setup[b]

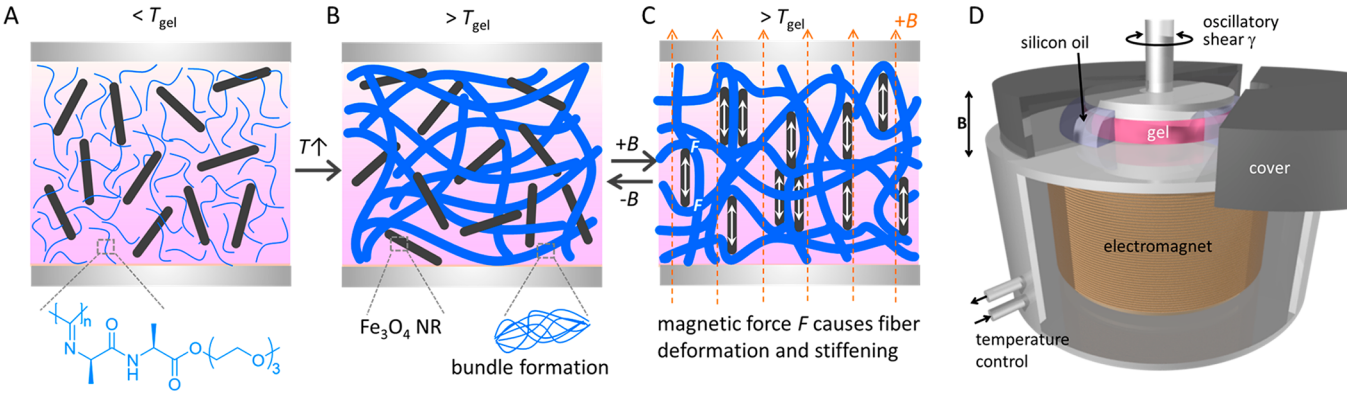

[a](A) Precooled PIC polymer (blue) and MIONR (black) solutions are mixed and placed between the plates below T_{gel}. (B) Heating the hybrids above T_{gel} induces polymer bundling into a semiflexible fibrous network with the MIONRs randomly dispersed. (C) In the presence of an external magnetic field, the particles align along the direction of the field and interact to induce fiber deformation, which results in stiffening. [b]The gel sample is formed between a plate and TA Instruments' temperature-controlled magnetorheology accessory with the magnetic field (maximum **B** = 1 T) directed perpendicular to the shear direction.

synthetic and therefore highly tailorable in properties. The thermoreversible PIC gels have developed into a valuable *in vitro* research tool,[27−29] which also shows promising results in *in vivo* studies.[30,31] For the magnetic components, we study the effect of differently shaped ferromagnetic magnetite (Fe_3O_4) particles (Figure 1A–C, Supporting Information Figure S1): magnetic iron oxide nanorods (MIONRs, diameter 48 nm, length 424 nm), large magnetic iron oxide nanospheres (LMIONSs, diameter 302 nm), and small magnetic iron oxide nanospheres (SMIONSs, diameter 37 nm). Note that the diameters of the nanospheres correspond approximately to the diameter and length of the nanorods. The synthesis of the PIC polymer[32,33] and water-dispersible magnetite particles[34−36] is described in detail in the Supporting Information.

The ferrogels were prepared by mixing a cold PIC solution with an aqueous precooled well-dispersed nanoparticle solution (Scheme 1A), followed by heating the mixture to 37 °C (Scheme 1B, Supporting Information for details). When the temperature surpasses the PIC gelation temperature (T_{gel} ≈ 16 °C, Figure S3), bundling of PIC chains is formed, which creates a network wherein the magnetic particles are randomly dispersed (Scheme 1B). In the presence of the magnetic field (Scheme 1C), the particles align and interact, which induces the fiber deformation. As the PIC gel is stress-stiffening, the stiffness increases when the nanoparticles respond to the magnetic field. For all particles, the formation of a ferrogel is clear from magnetic guidance experiments (Movies S1, S2).

Magnetorheology Experiments. The magnetic stiffening experiments were carried out on a stress-controlled rheometer equipped with a magnetic field accessory (Scheme 1D), which can apply fields up to 1 T perpendicular to the shear direction. The gels are formed between (parallel) rheometer plates, and

https://doi.org/10.1021/acs.nanolett.1c00371
Nano Lett. 2021, 21, 6740−6747

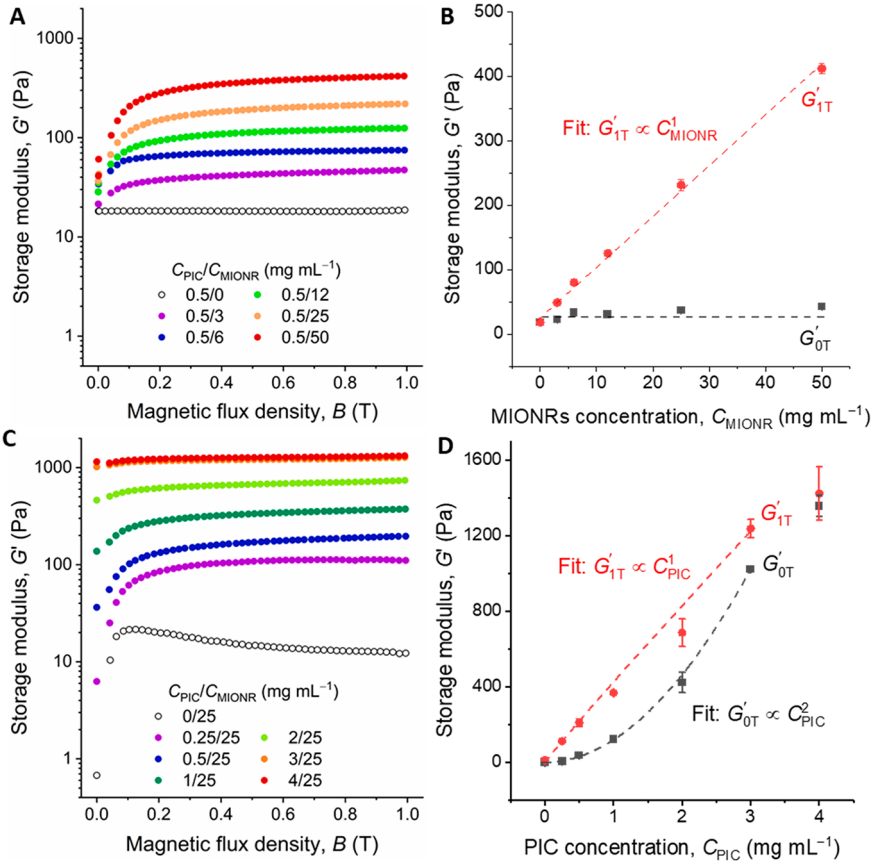

Figure 2. Stiffening of the PIC/MIONR hybrids. (A) Shear modulus G' of hybrids with different C_{MIONR} (at C_{PIC} = 0.5 mg mL^{-1}) as a function of magnetic flux density (T = 37 °C). Note that the stiffening response is still not saturated at C_{MIONR} > 50 mg mL^{-1}. (B) Storage moduli as a function of C_{MIONR} in the absence and the presence of a 1 T magnetic field. G'_{1T} scales linearly with C_{MIONR}. (C) Shear modulus G' of hybrids with different C_{PIC} (at C_{MIONR} = 25 mg mL^{-1}) as a function of magnetic flux density (T = 37 °C). (D) Storage moduli as a function of C_{PIC} in the absence and the presence of a 1 T magnetic field. G'_{1T} scales linearly with C_{PIC} below C_{PIC} = 3 mg mL^{-1}. Note that the G'_{0T} scales stronger with the PIC concentration: $G'_{0T} \propto C^2_{PIC}$.

the mechanical properties, in the absence or presence of an external magnetic field, are probed with a small shear strain. After gel formation at 37 °C, the application of a small magnetic field (∼100 mT) strongly stiffens the hybrids. At further increasing fields, the stiffening response levels off (Figure 1D). Note that also the corresponding ferrofluids (i.e., the dispersion of the magnetic nanoparticles in absence of the PIC gel) show an increased shear modulus but to a much less extent (Figure S2). Contrarily, PIC gels without magnetite particles do not stiffen (or soften) in the presence of a magnetic field.

We hypothesized that the strong experimentally observed magnetostiffening effect originates from reorientation and interaction of the Fe_3O_4 particles, which is transduced to the strain-sensitive fibrous network of the PIC gel (Scheme 1C). As such, hydrogels based on polyacrylamide (PAAM) that are composed of networks of flexible polymer chains are not expected to show any effect. Indeed, PAAM gels with a similar shear modulus with or without loading of magnetic nanoparticles show no response to the magnetic field (Figure 1D). Earlier work showed that 6-fold stiffening of PAAM gels loaded with carbonyl iron particles can only be achieved at high particle concentrations (20 wt %) at similar magnetic fields; such concentrations render the composites only suitable for 2D cell culture studies.[23] In addition, we emphasize that the PIC-based hybrids do not contract during application of the magnetic field (Figures S6, S7 and Movie S3) and do not leak from the hydrogel (Figure S11), highlighting that stiffening is not simply the result of matrix densification and that this strategy may be suitable for 3D cell culture experiments.

We then compare the shape and size of the particles (Figure 1D); we observe that at the same particle weight fraction (25 mg mL^{-1}), SMIONSs show the smallest magnetically induced stiffening response G'_{1T}/G'_{0T} = 5.0; the stiffening response of the LMIONSs (10.7) and of the MIONRs (11.8) is similar. The latter result indicates that magnetic torques have a minor contribution to the stiffening response and that the stiffening mechanism can be mainly attributed to the stress-stiffening character of the PIC matrix, which may allow for extrapolation of our results to other semiflexible fibrous networks doped with magnetic (nano)particles.

The literature indicates that larger particles and particles with larger aspect ratios are less toxic to cells because of the reduced uptake efficacy by avoiding cell wall penetration or membrane damage.[37,38] Considering the expected viability, combined with the fact that the stiffening for both MIONRs and LMIONSs is nearly the same, we focus in the remainder of this manuscript on the application of the Fe_3O_4 nanorods.

Final characteristics of our PIC-transduced magnetic stiffening mechanism are the rate and the reversibility of the process. As the stiffening does not depend on architectural changes inside the network (Figure S5B), we find that the

https://doi.org/10.1021/acs.nanolett.1c00371
Nano Lett. 2021, 21, 6740−6747

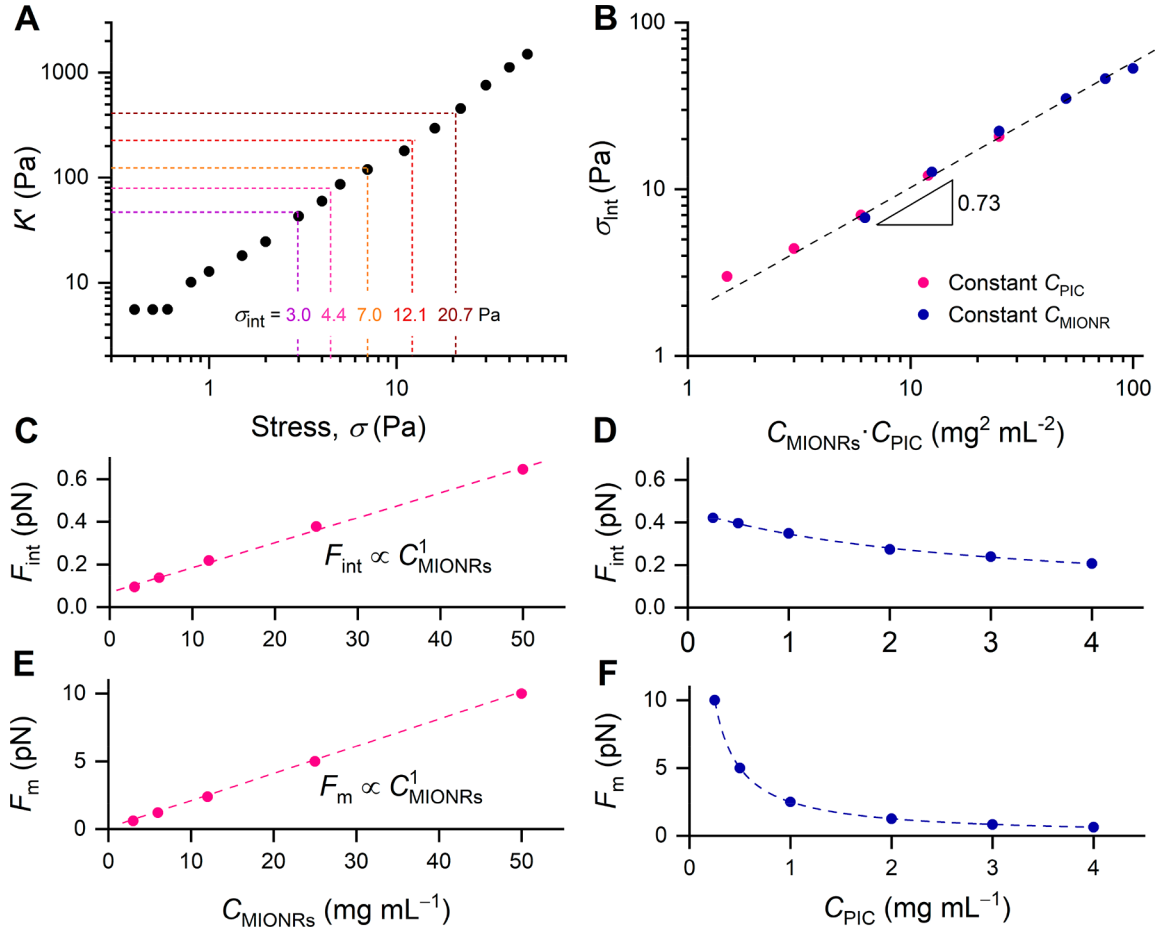

Figure 3. (A) Differential modulus K' as a function of external prestress σ for PIC gel without MIONRs (C_{PIC} = 0.5 mg mL^{-1}, T = 37 °C). The dotted lines correspond to the modulus of the PIC/MIONR hybrids at magnetic field B = 1 T. (B) All experimental samples collapse on a master curve when σ_{int} is plotted against the product C_{MIONR}·C_{PIC}. The dashed line is a power law fit to the experimental data with a slope of 0.73. (C,D) The internal force in the network, averaged per fiber, F_{int} calculated from the stiffening response (eqs S2 and S3) as a function of C_{MIONR} and C_{PIC}. F_{int} scales linearly with C_{MIONR} and decreases slightly with increasing C_{PIC} (line is a guide to the eye). (E,F) The magnetic force exerted by the MIONRs, averaged per network fiber as a function of C_{MIONR} and C_{PIC}. F_m scales linearly with C_{MIONR} and decreases with increasing C_{PIC} (line is a guide to the eye).

response is very fast (Figure 1E). After a 200 mT field is applied, the stiffness increase is completed within 6 s, and the first data point is recorded, which allows for full temporal control of the mechanical properties. Moreover, the process is fully reversible; as soon as the field is removed, the stiffness returns, albeit somewhat slower. A magnetic field cycle experiment (19 times with a 200 mT field 10 min on and 10 min off) shows full stability for several hours, which gives access to dynamically changing the mechanical properties of the hydrogel.

Effects of Nanoparticle and Polymer Concentration. The stiffening mechanism discussed so far is attributed to the complementary response of the magnetic-field-responsive MIONPs and stress-responsive PIC. Consequently, the concentration of both components is expected to affect the stiffening. Indeed, stiffening increases with the MIONR concentration, C_{MIONR} (Figures 2A and S9A). In the absence of a magnetic field, the particle concentration has a negligible effect on the gel stiffness, but at a field of 1 T, we observe that magnetic stiffening increases linearly with the MIONR concentration $G'_{1T} \propto C^{1.0}_{MINOR}$ (Figures 2B, S8C,D). The relation even holds for nanorod concentrations as low as 3 mg mL^{-1}.

As can be expected, when the PIC concentration, C_{PIC}, is increased, the stiffness of the hybrid gels in the magnetic field also increases (Figure 2C). At the same time, the stiffness of the hybrids in the absence of the field show a stronger increase, $G'_{0T} \propto C^2_{PIC}$, which follows the models for semiflexible polymers. Quantitative analysis shows the linear scaling relation $G'_{1T} \propto C^{1.0}_{MINOR}$ (Figure 2D), and we find a crossover at C_{PIC} > 3 mg mL^{-1}. At this concentration, the MIONRs (at 25 mg mL^{-1}) are no longer able to stiffen the network (Figure S8F). Note that the strongest relative stiffening is observed at low PIC concentration: for C_{PIC} = 0.25 mg mL^{-1}, we find a stiffening G'_{1T}/G'_{0T} = 18. At typical cell culture concentrations of C_{PIC} = 1 or 2 mg mL^{-1} (and C_{MIONR} = 25 mg mL^{-1}), the stiffening ratio $G'_{1T}/G'_{0T} \approx 4$ and 2, respectively.[27,29,33]

Earlier work on magnetically induced stiffening of soft materials that studied (spherical) magnetic micro/nanoparticles proposed two distinct steps in particle reorganization; first particles quickly align into chains, which then assemble into aggregates at a slower rate.[39] In our case, both processes are expected to contribute to PIC stiffening, with a major difference that we do not expect full aggregation of the nanoparticles, since they are encapsulated in the PIC network, and the particles are expected to merely interact. Stiffening

https://doi.org/10.1021/acs.nanolett.1c00371
Nano Lett. 2021, 21, 6740−6747

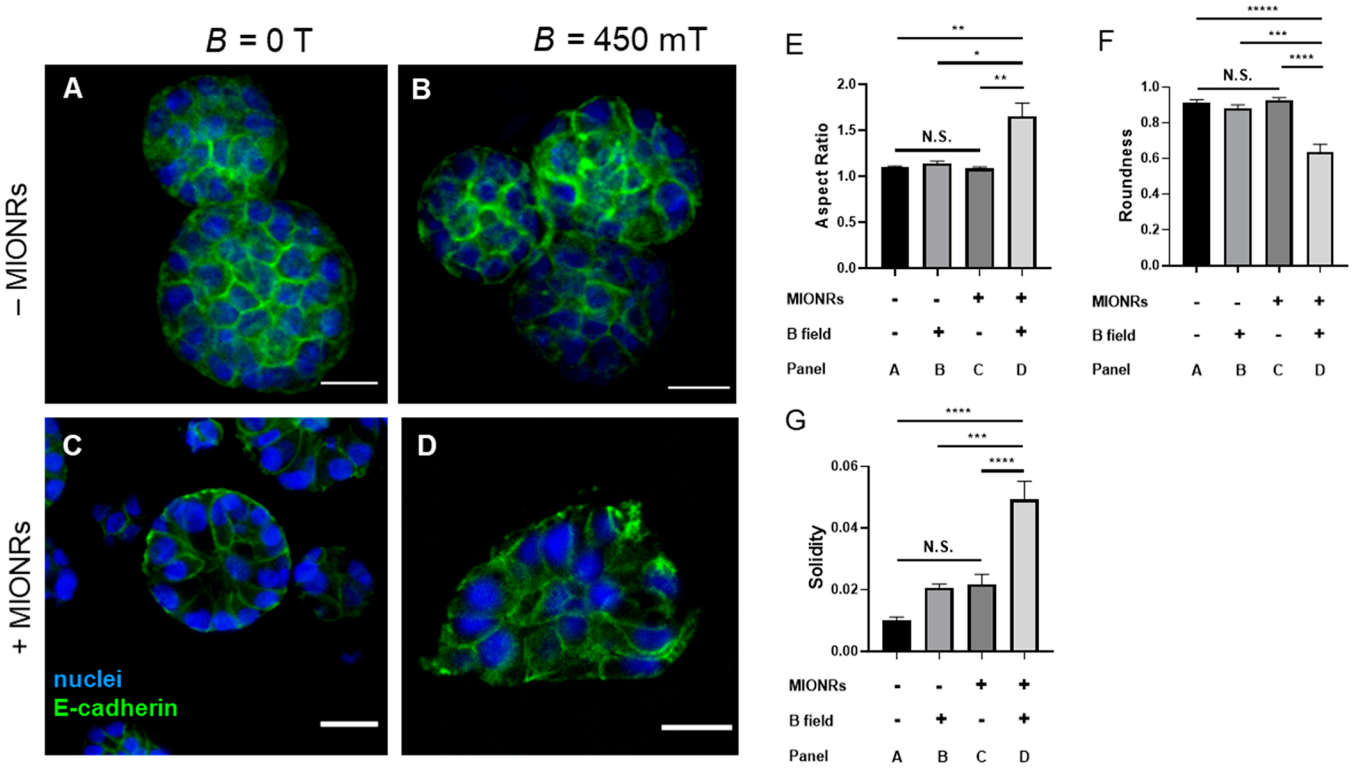

Figure 4. Effect of magnetomechanical stimulation on MCF10A cells 3 days after seeding. (A,B) Immunofluorescence imaging of mammary gland fragments cultured in PIC/Matrigel without MIONRs in the absence (A) and in the presence of a B = 450 mT magnetic field (B) with nuclei stained blue and E-cadherin stained green. Without MIONRs, the morphology of MCF10A cells is not affected by the field. (C,D) Immunofluorescence imaging of MCF10A clusters in PIC/Matrigel/MIONRs matrices in the absence (C) and in the presence of a B = 450 mT magnetic field (D). The morphology of MCF10A cells changed in the presence of both the MIONRs and the magnetic field. Scale bar: 20 μm. (E–G) The quantification of the morphology corresponding to the above four conditions by aspect ratio (E), roundness (F), and solidity (G).

experiments in sweeps where the field is ramped up to 1 T in a 5 min sweeps (Figure S10) show that the response quickly saturated, which indicates that both processes are relatively fast. For quantification, the experimental data was fitted to a two-term exponential decay model (Tables S2 and S3), analogous to earlier work.[39] We find that, indeed, particle alignment is fast (seconds time scale) and independent of MIONR or PIC concentrations. Secondary particle interaction, however is a slower process with a characteristic time scale that is concentration-dependent: it becomes faster at higher C_{MIONR} and slower at an increased PIC network density.

Quantification of Magnetic Forces and Forces inside the Network. We then aimed to study how efficient the magnetic forces generated by the MIONRs after application of the external field are transduced to mechanical forces and how much force is exerted in the network. Since local measurements are very difficult, we then calibrated the stresses generated by the MIONRs with the stress from an external (shear) deformation (Figure 3A). Despite the difference in origin between internal and external stress, the stiffening experiments are very comparable: in the strain-stiffening experiment, a continuous stress (or prestress) is applied that stiffens the material, which is quantified by a small superposed oscillatory stress; and in the magnetic stiffening, the external magnetic field causes the stiffening, which is similarly quantified by a small oscillatory stress. This stress calibration strategy has been used earlier to analyze network stresses in myosin-contracted actin gels[40] and in PIC gels stiffened by the thermoresponsive poly(*N*-isopropylacrylamide).[12] For the strain-stiffening experiment, we measure the differential modulus $K' = \delta\sigma/\delta\gamma$ (where $\delta\sigma$ and $\delta\gamma$ are the oscillatory stress and strain), which more accurately describes the stiffness of the material under an externally applied prestress. At low external strain or stress, $K' = G'$, but beyond a critical stress, σ_c, the stiffening regime is entered, where the modulus becomes dependent on the applied external prestress by $K' \propto \sigma^m$ where m is the stiffening index, which, theoretically,[41] is limited to $m \leq 3/2$. The parameters σ_c and m that describe the nonlinear mechanics both depend on polymer concentration; hence, strain-stiffening data was recorded for all PIC concentrations discussed in this manuscript.

We now can compare the modulus of the magnetically stiffened hydrogels (Figures 2B and 3A, dotted lines) to the strain-stiffening experiment (Figure 3A) and calibrate the stress that the magnetic particles induce with the stress applied by the rheometer to yield an average internal stress σ_{int}. Also, the magnetically induced stresses at different polymer concentrations were similarly calibrated. With all data taken together, we observe that σ_{int} in the magnetically stiffened gels collapses to a single master curve when plotted against the product of PIC and MIONR concentrations (Figure 3B, Table S1).

From the stress σ_{int}, and the mathematically determined fiber density, we calculate the internal force on an average PIC fiber, F_{int} (eqs S2, S3). As can be expected, F_{int} scales linearly to C_{MIONR} (Figure 3C) and weakly decreases with increasing C_{PIC} (Figure 3D). Quantitatively, the piconewton internal forces that are generated by the magnetic field are of a similar order of magnitude as the contractile forces of cells that stiffen a fibrin matrix.[40]

https://doi.org/10.1021/acs.nanolett.1c00371
Nano Lett. 2021, 21, 6740–6747

After the experimental analysis, we theoretically calculated whether the magnetic field that acts on the nanoparticles generates enough force to realize the observed effect. From the particle details and magnetic field gradient inside the rheometer setup, we calculated F_m, the maximum magnetic force that the nanorods can apply to an average fiber in the network (eqs S4−S13, details in Supporting Information). We find that F_m values (Figure 3E,F) are only about an order of magnitude higher than the calculated F_{int} levels in the network, which suggest that the magnetic forces from the MIONRs are effectively transduced into a stiffening response. Our quantitative theoretical analysis of force generation provides microscale insight, which serves as valuable input for the next generations of mechanotransductive biomaterials.

PIC/MIONR Composites as Adaptive Matrix Material. We then studied if the magnetic stiffening matrix fulfils its promise and can be used to change the mechanical properties in cell culture environments, in particular in a realistic 3D setting. First, cell viability tests were carried out on human foreskin fibroblasts to confirm that the MIONRs are not cytotoxic (Figure S13). Live−dead staining after culturing the cells for 72 h with the MIONRs (0−50 mg/mL) in the medium did not give any indication of toxicity. The fluorescent images show the presence of the nanorods close to the cell but it remains unclear if the nanoparticles have been internalized.

To demonstrate the effect of the in situ stiffening, we selected MCF10A cells, a mammary epithelial cell line that is commonly used in breast cancer models. MCF10A cells form clusters with different morphologies, dependent on the mechanical properties of their environment.[42] The clustering ensures the formation of a stable construct that can be visualized with traditional techniques after the strongly light-absorbing nanorods have been removed from the matrix (see Experimental Section). For cell adherence to the matrix, PIC was functionalized with the cell-binding peptide GRGDS (PIC-RGD). In addition, the PIC matrix was supplemented with basement membrane extract (Matrigel), which is critical for generating functional acini for MCF10A cells.[43] Functionalization and the addition of medium and Matrigel changes the linear and nonlinear mechanical properties of the matrix somewhat (decrease in G' and m), but the stiffening effect is still present (Figure S16). The cell culture matrix with MIONR (25 mg mL^{-1}) added stiffens a factor of 2.5 in the presence of a 450 mT magnetic field, and the stiffening response is not relaxing (Figure S17).

The MCF10A cells were seeded in PIC-RGD (2 mg mL^{-1}) both in the presence or absence of MIONRs (25 mg mL^{-1}), and the 3D cell cultures were placed in an incubator either on top of a permanent magnet ($B \approx 450$ mT, Figure S14) or away from the magnet.

Based on the work by the Chaudhuri lab,[42] we expected the mammary epithelial cells to display a more invasive morphology as a result of an increased matrix stiffness. Indeed, we find that MCF10A display growth-arrested acinar structures in the absence of MIONRs or a magnetic field (Figure 4A−C). Only in the presence of both the nanorods and the external field, their morphology changed to the invasive status (Figure 4D). The morphology change was quantified by determining the aspect ratio (Figure 4E), roundness (Figure 4F), and solidity (Figure 4G) of the cells (details in Supporting Information). The analysis shows significant differences for all three quantities of the experimental group (with MIONRs and an external magnetic field) compared to all controls. Note that we did not observe any significant differences between the control groups, i.e., the application of a magnetic field to the PIC/Matrigel matrix or the addition of the nanorods to the matrix without an external magnetic field has is not influencing the MCF10A cell cluster morphology. The ease of preparation (simply mixing in the particles) and application of the stimulus (placing on a commercially available permanent magnet) make these magnetoresponsive hydrogels available to any researcher who aims to study (temporal) mechanical effects on cell behavior.

CONCLUSIONS

In summary, we reported that PIC hydrogels doped with low concentrations of MIONRs show a strong magnetomechanical effect in the presence of very modest magnetic fields. The effect originates from rearrangement of the ferromagnetic nanorods, which is transduced to the strain-sensitive PIC gel. Our analysis indicates that forces generated inside these soft materials are comparable to contractile forces found in biology. Application of a magnetic field from a simple commercial permanent magnet is sufficient to change morphologies in an MCF10A cell culture experiment, which demonstrates that these hybrids are uniquely suited for 3D cell culture systems with on-demand adaptive mechanical properties. The magnetic field as a stimulus further offers the advantages of ease of use, remote control, strength modulation, and full penetration through the culture system, or even deep penetration *in vivo* (demonstrated by the development of MRI). Combined with the current attention for synthetic strain-stiffening hydrogels, we foresee broad application of magnetic stiffening in hydrogel platforms in, for instance, organoid development and the formation of complex tissue morphologies.

ASSOCIATED CONTENT

Supporting Information

The Supporting Information is available free of charge at https://pubs.acs.org/doi/10.1021/acs.nanolett.1c00371.

Synthetic procedures and materials characterization, additional mechanical data, relaxation data, magnetic field gradients, and images from cell culture experiments (PDF)

Movie S1. Movie of magnetic guiding of the composite with an external magnetif field (MP4)

Movie S2. Movie of magnetic guiding of the composite against gravity (MP4)

Movie S3. Movie showing that the composite does not contract (MP4)

AUTHOR INFORMATION

Corresponding Author

Paul H. J. Kouwer − *Radboud University, Institute for Molecules and Materials, 6525 AJ Nijmegen, The Netherlands;* orcid.org/0000-0002-2760-191X; Email: p.kouwer@science.ru.nl

Authors

Wen Chen − *Radboud University, Institute for Molecules and Materials, 6525 AJ Nijmegen, The Netherlands*

Ying Zhang − *Radboud University, Institute for Molecules and Materials, 6525 AJ Nijmegen, The Netherlands*

Jyoti Kumari − *Radboud University, Institute for Molecules and Materials, 6525 AJ Nijmegen, The Netherlands*

https://doi.org/10.1021/acs.nanolett.1c00371
Nano Lett. 2021, 21, 6740−6747

Hans Engelkamp − *Radboud University, Institute for Molecules and Materials, 6525 AJ Nijmegen, The Netherlands; Radboud University, High Field Magnet Laboratory (HFML-EMFL), 6525 ED Nijmegen, The Netherlands;* orcid.org/0000-0001-9920-0536

Complete contact information is available at: https://pubs.acs.org/10.1021/acs.nanolett.1c00371

Author Contributions

W.C. synthesized the polymers and magnetic nanomaterials and did the mechanical characterization. W.C., P.H.J.K., and H.E. analyzed the data. Y.Z. and J.K. did the cell culture. W.C. and P.H.J.K. wrote the manuscript. P.H.J.K. supervised the project.

Notes

The authors declare no competing financial interest.

■ ACKNOWLEDGMENTS

We thank TA Instruments for lending the magnetorheological accessory for the rheometer. W.C. acknowledges funding from the China Scholarship Council, grant number 201706260280. We thank Pieter Roelofs for helping in the experiments.

■ REFERENCES

(1) Van Helvert, S.; Storm, C.; Friedl, P. Mechanoreciprocity in cell migration. *Nat. Cell Biol.* **2018**, *20*, 8−20.
(2) Chakrabarti, R.; Celià-Terrassa, T.; Kumar, S.; Hang, X.; Wei, Y.; Choudhury, A.; Hwang, J.; Peng, J.; Nixon, B.; Grady, J. J.; et al. Notch ligand Dll1 mediates cross-talk between mammary stem cells and the macrophageal niche. *Science* **2018**, *360*, No. eaan4153.
(3) Loebel, C.; Mauck, R. L.; Burdick, J. A. Local nascent protein deposition and remodelling guide mesenchymal stromal cell mechanosensing and fate in three-dimensional hydrogels. *Nat. Mater.* **2019**, *18*, 883−891.
(4) Kharkar, P. M.; Kiick, K. L.; Kloxin, A. M. Designing degradable hydrogels for orthogonal control of cell microenvironments. *Chem. Soc. Rev.* **2013**, *42*, 7335−7372.
(5) Kratochvil, M. J.; Seymour, A. J.; Li, T. L.; Paşca, S. P.; Kuo, C. J.; Heilshorn, S. C. Engineered materials for organoid systems. *Nat. Rev. Mater.* **2019**, *4*, 606−622.
(6) Rosales, A. M.; Anseth, K. S. The design of reversible hydrogels to capture extracellular matrix dynamics. *Nat. Rev. Mater.* **2016**, *1*, 15012.
(7) Li, Z.; Fan, Z.; Xu, Y.; Lo, W.; Wang, X.; Niu, H.; Li, X.; Xie, X.; Khan, M.; Guan, J. pH-sensitive and thermosensitive hydrogels as stem-cell carriers for cardiac therapy. *ACS Appl. Mater. Interfaces* **2016**, *8*, 10752−10760.
(8) Kocak, G.; Tuncer, C.; Bütün, V. pH-Responsive polymers. *Polym. Chem.* **2017**, *8*, 144−176.
(9) Bao, X.; Si, X.; Ding, X.; Duan, L.; Xiao, C. pH-responsive hydrogels based on the self-assembly of short polypeptides for controlled release of peptide and protein drugs. *J. Polym. Res.* **2019**, *26*, 278.
(10) Thérien-Aubin, H. l.; Wang, Y.; Nothdurft, K.; Prince, E.; Cho, S.; Kumacheva, E. Temperature-responsive nanofibrillar hydrogels for cell encapsulation. *Biomacromolecules* **2016**, *17*, 3244−3251.
(11) Rombouts, W. H.; de Kort, D. W.; Pham, T. T.; van Mierlo, C. P.; Werten, M. W.; de Wolf, F. A.; van der Gucht, J. Reversible temperature-switching of hydrogel stiffness of coassembled, silk-collagen-like hydrogels. *Biomacromolecules* **2015**, *16*, 2506−2513.
(12) de Almeida, P.; Jaspers, M.; Vaessen, S.; Tagit, O.; Portale, G.; Rowan, A. E.; Kouwer, P. H. J. Cytoskeletal stiffening in synthetic hydrogels. *Nat. Commun.* **2019**, *10*, 609.
(13) Tang, L.; Gong, L.; Zhou, G.; Liu, L.; Zhang, D.; Tang, J.; Zheng, J. Design of low temperature-responsive hydrogels used as a temperature indicator. *Polymer* **2019**, *173*, 182−189.
(14) Accardo, J. V.; Kalow, J. A. Reversibly tuning hydrogel stiffness through photocontrolled dynamic covalent crosslinks. *Chem. Sci.* **2018**, *9*, 5987−5993.
(15) Lin, P.; Ma, S.; Wang, X.; Zhou, F. Molecularly engineered dual-crosslinked hydrogel with ultrahigh mechanical strength, toughness, and good self-recovery. *Adv. Mater.* **2015**, *27*, 2054−2059.
(16) Rosales, A. M.; Vega, S. L.; DelRio, F. W.; Burdick, J. A.; Anseth, K. S. Hydrogels with reversible mechanics to probe dynamic cell microenvironments. *Angew. Chem., Int. Ed.* **2017**, *56*, 12132−12136.
(17) Li, L.; Scheiger, J. M.; Levkin, P. A. Design and applications of photoresponsive hydrogels. *Adv. Mater.* **2019**, *31*, 1807333.
(18) Yuan, H.; Zhan, Y.; Rowan, A. E.; Xing, C.; Kouwer, P. H. J. Biomimetic Networks with Enhanced Photodynamic Antimicrobial Activity from Conjugated Polythiophene/Polyisocyanide Hybrid Hydrogels. *Angew. Chem.* **2020**, *132*, 2742−2746.
(19) Zhang, N.; Lock, J.; Sallee, A.; Liu, H. Magnetic nanocomposite hydrogel for potential cartilage tissue engineering: synthesis, characterization, and cytocompatibility with bone marrow derived mesenchymal stem cells. *ACS Appl. Mater. Interfaces* **2015**, *7*, 20987−20998.
(20) Tay, A.; Sohrabi, A.; Poole, K.; Seidlits, S.; Di Carlo, D. A 3D magnetic hyaluronic acid hydrogel for magnetomechanical neuromodulation of primary dorsal root ganglion neurons. *Adv. Mater.* **2018**, *30*, 1800927.
(21) Mitsumata, T.; Honda, A.; Kanazawa, H.; Kawai, M. Magnetically tunable elasticity for magnetic hydrogels consisting of carrageenan and carbonyl iron particles. *J. Phys. Chem. B* **2012**, *116*, 12341−12348.
(22) Ghadban, A.; Ahmed, A. S.; Ping, Y.; Ramos, R.; Arfin, N.; Cantaert, B.; Ramanujan, R. V.; Miserez, A. Bioinspired pH and magnetic responsive catechol-functionalized chitosan hydrogels with tunable elastic properties. *Chem. Commun.* **2016**, *52*, 697−700.
(23) Abdeen, A. A.; Lee, J.; Bharadwaj, N. A.; Ewoldt, R. H.; Kilian, K. A. Temporal modulation of stem cell activity using magnetoactive hydrogels. *Adv. Healthcare Mater.* **2016**, *5*, 2536−2544.
(24) Tasoglu, S.; Kavaz, D.; Gurkan, U. A.; Guven, S.; Chen, P.; Zheng, R.; Demirci, U. Paramagnetic levitational assembly of hydrogels. *Adv. Mater.* **2013**, *25*, 1137−1143.
(25) Kouwer, P. H. J.; Koepf, M.; Le Sage, V. A. A.; Jaspers, M.; van Buul, A. M.; Eksteen-Akeroyd, Z. H.; Woltinge, T.; Schwartz, E.; Kitto, H. J.; Hoogenboom, R.; Picken, S. J.; Nolte, R. J. M.; Mendes, E.; Rowan, A. E. Responsive biomimetic networks from polyisocyanopeptide hydrogels. *Nature* **2013**, *493*, 651−655.
(26) Storm, C.; Pastore, J. J.; MacKintosh, F. C.; Lubensky, T. C.; Janmey, P. A. Nonlinear elasticity in biological gels. *Nature* **2005**, *435*, 191−194.
(27) Zhang, Y.; Tang, C.; Span, P. N.; Rowan, A. E.; Aalders, T. W.; Schalken, J. A.; Adema, G. J.; Kouwer, P. H. J.; Zegers, M. M. P.; Ansems, M. Polyisocyanide Hydrogels as a Tunable Platform for Mammary Gland Organoid Formation. *Adv. Sci.* **2020**, *7*, 2001797.
(28) Ye, S.; Boeter, J. W. B.; Mihajlovic, M.; van Steenbeek, F. G.; van Wolferen, M. E.; Oosterhoff, L. A.; Marsee, A.; Caiazzo, M.; van der Laan, L. J. W.; Penning, L. C.; Vermonden, T.; Spee, B.; Schneeberger, K. A Chemically Defined Hydrogel for Human Liver Organoid Culture. *Adv. Funct. Mater.* **2020**, *30*, 2000893.
(29) Das, R. K.; Gocheva, V.; Hammink, R.; Zouani, O. F.; Rowan, A. E. Stress-stiffening-mediated stem-cell commitment switch in soft responsive hydrogels. *Nat. Mater.* **2016**, *15*, 318−325.
(30) Op 't Veld, R. C.; van den Boomen, O. I.; Lundvig, D. M. S.; Bronkhorst, E. M.; Kouwer, P. H. J.; Jansen, J. A.; Middelkoop, E.; Von den Hoff, J. W.; Rowan, A. E.; Wagener, F. Thermosensitive biomimetic polyisocyanopeptide hydrogels may facilitate wound repair. *Biomaterials* **2018**, *181*, 392−401.
(31) Wang, B.; Booij-Vrieling, H. E.; Bronkhorst, E. M.; Shao, J.; Kouwer, P. H. J.; Jansen, J. A.; Walboomers, X. F.; Yang, F. Antimicrobial and anti-inflammatory thermo-reversible hydrogel for periodontal delivery. *Acta Biomater.* **2020**, *116*, 259−267.

(32) Koepf, M.; Kitto, H. J.; Schwartz, E.; Kouwer, P. H. J.; Nolte, R. J. M.; Rowan, A. E. Preparation and characterization of non-linear poly (ethylene glycol) analogs from oligo (ethylene glycol) functionalized polyisocyanopeptides. *Eur. Polym. J.* **2013**, *49*, 1510−1522.
(33) Liu, K.; Mihaila, S. M.; Rowan, A.; Oosterwijk, E.; Kouwer, P. H. J. Synthetic Extracellular Matrices with Nonlinear Elasticity Regulate Cellular Organization. *Biomacromolecules* **2019**, *20*, 826−834.
(34) Lou, L.; Yu, K.; Zhang, Z.; Huang, R.; Zhu, J.; Wang, Y.; Zhu, Z. Dual-mode protein detection based on Fe3O4-Au hybrid nanoparticles. *Nano Res.* **2012**, *5*, 272−282.
(35) Hong, Y.; Shi, H.; Shu, X.; Zheng, Y.; Zhang, Y.; Wu, Y. Controlled synthesis of hollow magnetic Fe3O4 nanospheres: Effect of the cooling rate. *Particuology* **2017**, *33*, 24−28.
(36) Xu, W.; Wang, M.; Li, Z.; Wang, X.; Wang, Y.; Xing, M.; Yin, Y. Chemical transformation of colloidal nanostructures with morphological preservation by surface-protection with capping ligands. *Nano Lett.* **2017**, *17*, 2713−2718.
(37) Tarantola, M.; Pietuch, A.; Schneider, D.; Rother, J.; Sunnick, E.; Rosman, C.; Pierrat, S.; Soennichsen, C.; Wegener, J.; Janshoff, A. Toxicity of gold-nanoparticles: synergistic effects of shape and surface functionalization on micromotility of epithelial cells. *Nanotoxicology* **2011**, *5*, 254−268.
(38) Simon-Deckers, A.; Loo, S.; Mayne-L'hermite, M.; Herlin-Boime, N.; Menguy, N.; Reynaud, C.; Gouget, B.; Carriere, M. Size-, composition-and shape-dependent toxicological impact of metal oxide nanoparticles and carbon nanotubes toward bacteria. *Environ. Sci. Technol.* **2009**, *43*, 8423−8429.
(39) An, H.; Picken, S. J.; Mendes, E. Enhanced hardening of soft self-assembled copolymer gels under homogeneous magnetic fields. *Soft Matter* **2010**, *6*, 4497−4503.
(40) Koenderink, G. H.; Dogic, Z.; Nakamura, F.; Bendix, P. M.; MacKintosh, F. C.; Hartwig, J. H.; Stossel, T. P.; Weitz, D. A. An active biopolymer network controlled by molecular motors. *Proc. Natl. Acad. Sci. U. S. A.* **2009**, *106*, 15192−15197.
(41) Jaspers, M.; Dennison, M.; Mabesoone, M. F.; MacKintosh, F. C.; Rowan, A. E.; Kouwer, P. H. Ultra-responsive soft matter from strain-stiffening hydrogels. *Nat. Commun.* **2014**, *5*, 5808.
(42) Chaudhuri, O.; Koshy, S. T.; Branco da Cunha, C.; Shin, J.-W.; Verbeke, C. S.; Allison, K. H.; Mooney, D. J. Extracellular matrix stiffness and composition jointly regulate the induction of malignant phenotypes in mammary epithelium. *Nat. Mater.* **2014**, *13*, 970−978.
(43) Qu, Y.; Han, B.; Yu, Y.; Yao, W.; Bose, S.; Karlan, B. Y.; Giuliano, A. E.; Cui, X. Evaluation of MCF10A as a Reliable Model for Normal Human Mammary Epithelial Cells. *PLoS One* **2015**, *10*, No. e0131285.

https://doi.org/10.1021/acs.nanolett.1c00371
Nano Lett. 2021, 21, 6740−6747